

TinyRS-R1: Compact Multimodal Language Model for Remote Sensing

Aybora Köksal
aybora@metu.edu.tr

A. Aydin Alatan
alatan@metu.edu.tr

Center for Image Analysis (OGAM),
Department of Electrical and
Electronics Engineering
Middle East Technical University
Ankara, Turkey

Abstract

Remote-sensing applications often run on edge hardware that cannot host today’s 7B-parameter multimodal language models. This paper introduces TinyRS, the first 2B-parameter multimodal small language model (MSLM) optimized for remote sensing tasks, and TinyRS-R1, its reasoning-augmented variant. Built upon Qwen2-VL-2B, TinyRS is trained through a four-stage pipeline: pre-training on million satellite images, instruction tuning on visual instruction examples, fine-tuning with Chain-of-Thought (CoT) annotations from the proposed reasoning dataset, and alignment via Group Relative Policy Optimization (GRPO). TinyRS-R1 achieves or surpasses the performance of recent 7B-parameter remote sensing models across classification, VQA, visual grounding, and open-ended question answering—while requiring just one-third of the memory and latency. Our analysis shows that CoT reasoning substantially benefits spatial grounding and scene understanding, while the non-reasoning TinyRS excels in concise, latency-sensitive VQA tasks. TinyRS-R1 represents the first domain-specialized MSLM with GRPO-aligned CoT reasoning for general-purpose remote sensing. Code, models, and the captions for datasets will be released.

Introduction

Large and multimodal language models (LLMs and MLLMs) [1, 2, 25, 37, 43, 44] have recently redefined both natural language and visual understanding with models like GPT-4V [32] and open alternatives such as Qwen2-VL [48] and InternVL2 [8] setting new benchmarks in vision-language processing. Still, their general-purpose nature and computational burden pose challenges for specialized or resource-limited deployments. These improvements have sparked growing interest in Small Language Models (SLMs – Language Models with <3B parameters) [1, 24, 41, 42, 43] and their multimodal counterparts (MSLMs) [1, 2, 10, 20, 48]. This shift also leads to the introduction of domain-specialized models for the fields that require expertise, such as medicine [6] and chemistry [27], where the general-purpose models often fall short.

Remote Sensing (RS) is also one of the areas that requires domain specialization due to having different nature than regular imagery. Following the success of MLLMs in visual tasks, recent research has begun to adapt them to remote sensing image analysis. With

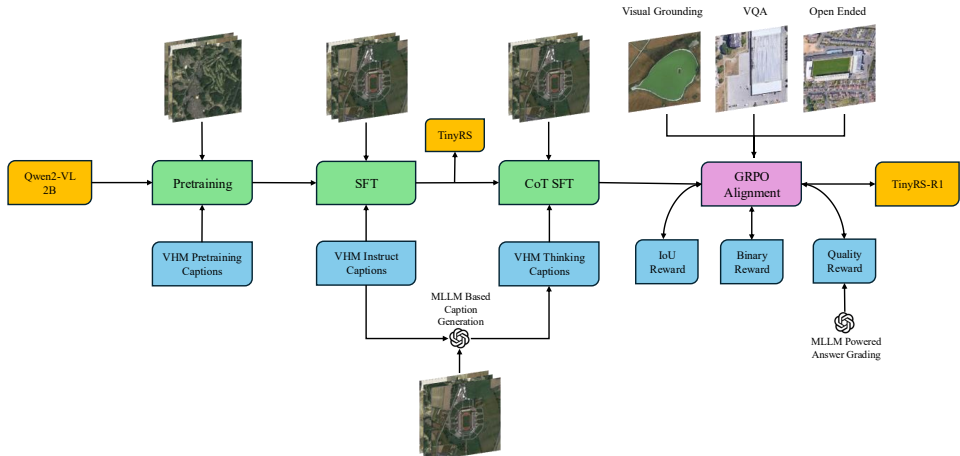


Figure 1: Training flowchart of the proposed models, TinyRS and TinyRS-R1.

the introduction of newer pre-training and introduction datasets, several recent MLLMs tailored for remote sensing [4, 10, 21, 28, 36, 53] have been developed to address core vision-language tasks, including visual question answering, object detection, and grounding within satellite imagery contexts. These advances highlight the growing impact of MLLMs in enhancing semantic and spatial understanding for satellite imagery analysis. However, all having 7B parameters, none of these models are counted as MSLMs and they are inapplicable for resource-limited edge devices. Moreover, these models do not take advantage of the alignment abilities of reinforcement learning in chain-of-thought reasoning, apart from very recent [21, 29] preprints, which we acknowledge as concurrent works.

Improving accuracy on complex tasks often relies on chain-of-thought prompting [30, 31], which guides models through intermediate steps. To reduce error propagation, reinforcement learning and step-level supervision have been used to enhance reliability [24, 45, 47]. These advances appear in proprietary models like OpenAI’s o-series [48, 49] and open-source systems such as DeepSeek-R1 [10], which leverage Group Relative Policy Optimization (GRPO) [39]—a reinforcement learning algorithm that equips compact multimodal models with strong reasoning capabilities [11, 19, 27].

To address the shortage of a small reasoning model for general RS problems, in this work, TinyRS model family is introduced. Trained in VHM [26] pre-training and visual instruction datasets, TinyRS either matches or outperforms existing models in most of known VQA, classification and visual grounding datasets, despite its much smaller parameter size. GRPO powered version of the model, TinyRS-R1 increases the performance even further, achieving state-of-the-art. For TinyRS to gain an ability to make a proper reasoning before giving an answer, it needs to be tuned with sample reasoning data. For this, *visual reasoning instructions* are proposed for VHM visual instruction dataset.

The contributions of this paper are as follows:

- We introduce TinyRS, to our knowledge, the smallest open source general purpose remote sensing MSLM, powered by Qwen2-VL.
- We propose VHM-Instruct-Think, visual reasoning captions for VHM dataset, which is, to our knowledge, first for RS literature.

- Fine-tuned with reasoning captions then aligned with GRPO, we introduce TinyRS-R1, the first reasoning based MSLM for solving general RS tasks.
- Throughout rigorous experiments, we show that both TinyRS and TinyRS-R1 outperforms or matches the existing state-of-the-art RS MLLMs in most of the popular RS metrics for language models, even the ones with much larger parameter sizes.

2 Related Work

LLMs. The Transformer architecture [46] enabled major LLM advances via BERT [12] and GPT [32], leading to models like GPT-3 [7]. LLaMA [42] showed smaller models can outperform larger ones, inspiring open LLMs such as Qwen [8], InternLM [43], and Gemma [41]. CLIP [38] sparked MLLMs like GPT-4V [5], Qwen-VL [9], and PaliGemma [5]. This evolution led to efficient sub-7B MSLMs, including PaliGemma 2 [40] and Qwen2-VL-2B [33]. Originally designed as general tools, MSLMs have shown that smaller, task-tuned models can outperform larger generalist ones in both accuracy and efficiency [8, 51].

Chain of Thought (CoT) Reasoning. Reasoning in large language models (LLMs) stems from Chain-of-Thought (CoT) prompting [14, 31, 49, 30, 52], which improves multi-step problem-solving via intermediate steps. Multimodal variants like Multimodal CoT [54], Visual Sketchpad [18], and Visualization-of-Thought [52] extend this to visual inputs for cross-modal reasoning. Reinforcement learning advances this further, as seen in OpenAI’s o-series [33, 35] and DeepSeek-R1 [15], which addresses language mixing via staged training and cold-start data. It employs Group Relative Policy Optimization (GRPO) [39] and enables distillation for scalable, self-improving reasoning across models from 1.5B to 70B. Despite these advances, many reasoning models remain general-purpose and lack task-specific fine-tuning. While OpenAI’s o-series supports multimodal reasoning, DeepSeek-R1 currently does not; however, GRPO opens the door for building domain-specific, multimodal reasoning models from open-source LLMs and MLLMs [10, 19, 27].

Remote Sensing MLLMs. Building on the success of multimodal large language models (MLLMs) in visual tasks, recent work has extended their use to remote sensing. Models like RSGPT [16] and GeoChat [21] introduced benchmarks (RSICap, RSIEval) and large instruction datasets with LoRA-based tuning [15] for tasks such as captioning, VQA, and spatial interaction. EarthGPT [5] unified multimodal inputs (optical, SAR, infrared), while RS-LLaVA [9] improved multi-task performance via LoRA. LHRS-Bot [28] and its successor LHRS-Bot-Nova [29] focused on geographic reasoning using datasets like LHRS1-Align and LHRS-Instruct. VHM [26] introduced a large-scale RS pretraining corpus with over 1M images and 178k instructions. Despite these advances, none introduces reinforcement learning (RL) for reasoning.

Two concurrent works attempt this: Muhtar *et al.* [29] introduce the 7B ScoreRS model for answer quality analysis, employing Qwen2-VL-RS and Qwen2-VL-RS-R1 with GRPO-based rewards. However, their reported improvements are modest compared to ours. We attribute our higher gains to the generalization ability of a smaller model, the use of higher-quality captions from GPT-4.1-mini, and our four-stage pipeline with continuous rewards and dataset balancing. As Muhtar *et al.*’s work is very recent and lacks complete training details and code—especially regarding the datasets used for CoT fine-tuning and RL—we were unable to fully reproduce their process using either their data or ours, though we did evaluate their released model for comparison. In contrast, MilChat [20] applies RL to military base

classification with strong results, but its scope is limited to a single remote sensing (RS) task, making it unsuitable for broader RS classification, VQA, or grounding, and thus not directly comparable to our approach.

3 Dataset

Throughout all training stages, both remote sensing (RS) pre-training images and visual instruction datasets from VHM [36] are used. During pre-training, original captions from the VHM dataset are directly employed using the entire pre-training set. For supervised fine-tuning, approximately 100K randomly selected images—over half of the VHM visual instruction dataset—are used. These include all RS tasks in VHM, such as Visual Question Answering, Visual Grounding, Scene Classification, Object Counting, Image Modality and Resolution Recognition, Geometric Measurement, Building Vectorization, and Multi-label Classification. In this work, this subset of the VHM visual instruction dataset is referred to as the VHM-Instruct dataset and is used throughout all fine-tuning stages.

Although Group Relative Policy Optimization (GRPO) can enhance the reasoning capabilities of any fine-tuned language model, its effectiveness is limited when applied in a cold-start setting without prior reasoning-based fine-tuning, especially with smaller language models [15, 20]. Additionally, since most VHM visual instruction captions contain only brief, often one-word or single-sentence responses, they are unsuitable for enabling Chain-of-Thought (CoT) reasoning. To address this, we introduce VHM-Instruct-Think, a set of reasoning-based captions generated for the VHM-Instruct dataset.

Reasoning captions are produced using OpenAI’s goal-oriented API model, GPT-4.1-mini [34]. The model is prompted with the image and VHM’s original question–answer pair alongside a detailed system message instructing it to simulate step-by-step CoT reasoning. The prompt encourages natural human-like thought processes with expressions like “*let me think*,” “*oh, I see*,” or “*but wait*,” and instructs the model not to reference the original answer directly during reasoning, treating it as metadata. The final format includes: `<reasoning> ... </reasoning> <answer> ... </answer>`. This approach enables the model to produce rich, descriptive reasoning while still generating concise, answer-aligned outputs (e.g., “yes” or “no”) suitable for downstream tasks.

For GRPO training, another subset of 10K randomly selected images—disjoint from the VHM-Instruct set—is used from the VHM visual instruction dataset. The question–answer pairs in this subset do not include any reasoning, as this dataset is not intended for use in the fine-tuning stage. This subset will be referred to as the VHM-RL dataset.

Samples from VHM-Instruct-Think dataset is provided in Figure 2.

4 Method

This study introduces TinyRS and TinyRS-R1 models, designed to leverage the capabilities of MLLMs for reasoning and captioning tasks on remote sensing imagery. This section details the architecture and training approach of TinyRS.

4.1 Model

TinyRS builds upon Qwen2-VL-2B [42], adopting both its architecture and pre-trained weights:

Question: Identify the location of a gray dam.

Thinking: User wants me to identify the location of a gray dam in this aerial or satellite image. A dam is a structure built across a river or stream to control the flow of water. It is a large body of water, likely a reservoir, surrounded by land with vegetation and some patches of farmland. The dam should be a linear structure located in the center of the image. Looking at the bottom part of the image, there is a long, straight, grayish structure that looks like a dam. This structure is surrounded by water on both sides. This contrasts with the natural landscape around it and appears to be man-made. This is a likely dam because it separates the water from the land and has a uniform gray surface. No other similar structures are visible in the image, so the most likely answer is this structure. The bounding box for this dam is approximately from the left-center to the right-center horizontally and covering the narrow strip between the two water bodies. The coordinates for this bounding box would start around the left side near 381 pixels horizontally and 825 pixels vertically, extending to about 878 pixels horizontally and 811 pixels vertically.

Visual Grounding

Answer: [0.381,0.625,0.876,0.811]

Question: Classify the image within one of the given classes: airplane, desert, mobile home park, ship, airport, forest, mountain, snowberg, baseball diamond, highway, overpass, stadium, beach, ground, rock field, parking lot, storage tank, bridge, tennis court, tennis court, chappal, industrial area, railway station, terrace, church, intersection, rectangular farmland, thermal power station, circular farmland, island, river, wetland, road, train, bridge, circular area, meadow, runway, dense residential, medium residential, residential, sea ice.

Thinking: User asks me to classify this image. Let me carefully analyze the image. I see a top-down aerial view showing a network of roads converging at a central point. There are multiple vehicles visible, indicating traffic flow. The roads are multi-lane, suggesting a highway or major road junction. Surrounding the roads are buildings and structures, suggesting an urban or semi-urban environment. The roads are well-defined and clearly visible. This strongly suggests this is a road intersection rather than a freeway, overpass, or roundabout, which have different structural layouts. It is not an airport, ship, or forest. The image is a top-down view, so there are no visible trees or mountains. The network with vehicles and buildings, so the best fitting class from the list is intersection.

Classification

Answer: intersection

Question: How many overpasses can you see in the image?

Thinking: User asks me how many overpasses can be seen in the image. Let me carefully analyze the image. I see a top-down aerial view of a highway with multiple lanes in each direction. There is a road crossing horizontally near the bottom of the image. The highway lanes do not pass over this horizontal road, as evidenced by the shadows and the visible edges of the elevated road. There are two separate bridge structures crossing over the horizontal road. These two separate bridge structures are side by side but distinct, and carrying traffic in one direction. This means there are two overpasses here, each containing one bridge. There are no other visible overpasses in the image. The other roads intersect at ground level with traffic signals and markings, but only the highway lanes pass over the horizontal road. Therefore, the total number of overpasses visible in the image is two.

Visual Question Answering

Answer: 2

Question: What type of transportation can be observed in the image?

Thinking: User asks me what types of transportation can be observed in the image. Let me carefully analyze the image step-by-step. First, I notice a dense urban area with many buildings and streets. The most prominent feature is a large highway with multiple lanes. There are also multiple parallel train tracks extending horizontally across the image. These tracks are clearly visible and indicate the presence of trains as a mode of transportation. Next, I look for other forms of transportation. I see several roads with vehicles on them, including ones which are scattered around the city blocks. The vehicles are mostly sedans, which are moving or parked, confirming that cars are also a mode of transportation in this area. So, the image shows a combination of transportation types: trains, evidenced by the extensive rail infrastructure and station, and cars, visible on the roads throughout the city. This suggests that both trains and cars serve as major modes of transportation in this urban environment.

Open Conversation

Answer: Both trains and cars serve as transportation means in the city, with numerous train tracks and a prominent train station in the center.

Figure 2: Sample image and question-reasoning-answer captions from proposed VHM-Instruct-Think dataset.

Visual Encoder: As in Qwen2-VL-2B, TinyRS employs a Vision Transformer (ViT) [10] with 675M parameters as its visual encoder. It supports naive dynamic resolution handling [11] during training and inference, enabling the model to accommodate inputs of varying image resolutions by dynamically transforming them into a variable number of visual tokens.

Language Model: The language backbone of TinyRS mirrors that of Qwen2-VL-2B, initialized from the pre-trained Qwen-1.5B model.

Position-Aware Vision-Language Adapter: To enhance computational efficiency, TinyRS integrates a vision-language adapter inspired by Qwen2-VL-2B. This adapter compresses visual features using a single-layer cross-attention mechanism, reducing the visual token sequence to a fixed size of 256. It preserves spatial relationships through 2D absolute positional encodings before passing the compressed features to the language model.

4.2 Training

Pre-training and Supervised Fine Tuning (SFT): The original Qwen2-VL-2B-Instruct model is fine-tuned in two stages to obtain the base TinyRS. In the first stage, the model is fine-tuned on VHM’s 1 million-image pre-training dataset. This pretrained model is then further fine-tuned using the VHM-Instruct dataset, as described in Section 3. Since some remote sensing tasks in VHM-Instruct are underrepresented, the dataset is balanced by increasing the sampling weight of these tasks—replicating certain examples up to five times per epoch. Through this fine-tuning procedure, even a relatively small 2B-parameter language model can achieve robustness across a wide range of remote sensing tasks. This two-stage training process yields the base TinyRS model.

Chain-of-Thought (CoT) Reasoning: To enhance interpretability and reliability, the model is trained to produce multi-step reasoning that explains the presence or absence of specific visual attributes, rather than providing direct answers. For example, instead of simply stating, “Yes, there is a white car,” the model first identifies visual elements—such as roads or object

positions—before concluding.

To enable this reasoning ability, the base TinyRS model is fine-tuned on the VHM-Instruct-Think dataset using Chain-of-Thought (CoT) prompting. As in previous fine-tuning stages, sampling weights are adjusted to balance underrepresented tasks. This equips the 2B-parameter MSLM with structured reasoning skills and aligns it more effectively with GRPO-based reinforcement learning.

Reinforcement Learning: In addition to supervised fine-tuning, a lightweight reinforcement learning (RL) phase is incorporated to better align the model’s outputs with classification objectives. Group Relative Policy Optimization (GRPO) is used to update the policy based on relative rewards computed over groups of generated responses. Inspired by DeepSeek-R1 [10], two types of rewards are introduced: format-based and accuracy-based.

The format-based reward is binary and granted if the model’s output adheres to the required structure: `<reasoning>...</reasoning> <answer>...</answer>`, regardless of what is written within the reasoning process and the final answer.

The accuracy-based reward is task-dependent:

- For closed-ended tasks (e.g., VQA, classification, multiple-choice), a binary reward (1 for correct, 0 for incorrect) is used.
- For visual grounding, which requires a bounding box as an output, the Intersection over Union (IoU) score is used as the reward.
- For open-ended tasks, GPT-4.1-mini serves as an automatic evaluator, scoring the model’s answer from 0 to 10. This score is then normalized to a [0.0, 1.0] range to provide a quality reward.

The policy is optimized with GRPO to increase the probability of high-reward outputs. GRPO is chosen over standard PPO for its sample efficiency and improved performance on reasoning tasks, reducing the number of required RL steps and mitigating the risk of model collapse or forgetting prior knowledge [10, 19].

Completing GRPO training with the VHM-RL dataset, the aforementioned four-stage training process yields the final TinyRS-R1 model. Alternatively, using the same dataset, GRPO can also be applied directly to a pretrained model—without any supervised fine-tuning—by training it with the specified reward function via reinforcement learning. This approach tests whether the model can learn purely from reward signals, starting from a “cold start” (as described in DeepSeek); its performance will be discussed as part of the ablation study.

5 Experiments

5.1 Settings

The training pipeline is built using PyTorch and the HuggingFace Transformers library, utilizing pretrained weights from Qwen2-VL models. All stages—including pre-training, supervised fine-tuning, and CoT fine-tuning—are conducted on high-performance computing (HPC) clusters equipped with $4 \times$ NVIDIA H100 GPUs (80GB HBM3), which are sufficient for full-parameter fine-tuning of the 2B model. Training is performed for one epoch using the Adam optimizer with an initial learning rate of 1×10^{-5} and a batch size of 16.

For the reinforcement learning phase, GRPO is implemented using the TRL (Transformer Reinforcement Learning) framework in a batched setting. This stage is executed on HPC clusters with $16 \times$ NVIDIA H100 GPUs, using the Adam optimizer with a starting learning rate of 1×10^{-6} , a batch size of 16, and 4 generated samples per image. Maximum prompt length and maximum completion length are increased to 8192. The GRPO training is also run for one epoch.

5.2 Results

Table 1: Performance of TinyRS on public RS benchmarks compared to previous models. The highest score in each benchmark is marked in **bold**, and the second is underlined.

Capability	Benchmark	TinyRS R1	TinyRS	VHM []	Qwen2-VL RS-R1 []	Qwen2-VL RS []	LHRS-Bot Nova []	GeoChat []
		thinking 2B	non-thinking 2B	non-thinking 7B	thinking 7B	non-thinking 7B	non-thinking 7B	non-thinking 7B
Remote Sensing Classification	AID	90.2	89.6	92.0	82.0	84.6	83.1	73.5
	METER-ML	72.1	65.1	74.3	69.4	72.2	<u>72.7</u>	34.8
	NWPU	<u>92.9</u>	92.0	94.8	84.0	86.7	83.9	89.4
	SIRI-WHU	76.8	66.9	70.6	70.3	74.6	72.3	53.1
	WHU-RS19	95.6	91.5	96.5	90.6	95.5	<u>96.2</u>	85.5
	Average	85.6	81.0	85.6	79.3	82.7	81.6	67.3
Remote Sensing Visual Question Answering	HR-Compare	73.5	80.6	83.4	77.5	80.3	89.1	<u>83.5</u>
	HR-Presence	<u>68.6</u>	64.5	62.6	64.0	66.3	84.0	57.3
	LR-Compare	84.0	89.9	90.3	82.8	89.1	88.2	90.7
	LR-Presence	78.1	90.4	89.9	74.1	86.4	84.6	<u>90.2</u>
	LR-Rural	76.0	<u>92.0</u>	89.0	74.0	76.0	68.0	96.0
	Average	76.0	83.5	83.0	74.5	79.6	82.8	83.5
RS Grounding	RSVG-DIOR	74.9	<u>69.4</u>	55.9	64.6	59.2	31.5	19.7
RS Gen. Know.	LHRS-Bench	56.8	57.4	33.0	69.2	<u>66.5</u>	52.5	36.2

Table 1 compares the proposed TinyRS family (2B parameters) with five recent 7B-scale remote-sensing MLLMs on four task groups: scene classification, visual question answering (VQA), grounding and general RS knowledge.

Most important key observations of Table 1 are as follows:

- In classification, TinyRS-R1 delivers the strongest average accuracy (85.6%) among all models, tying VHM while surpassing the other 7B baselines by 2–18 %. It also secures the best score on SIRI-WHU and second best on AID and WHU-RS19, demonstrating that lightweight CoT reasoning can capture subtle context cues without the heavy memory footprint of larger models. On the otherhand, base TinyRS reaches a respectable 81.0%, confirming that explicit reasoning is beneficial for fine-grained classification.
- The pattern reverses for VQA. Base TinyRS posts the highest overall accuracy (83.5%), matching GeoChat and exceeding every other competitor. Its concise, single-sentence answers align well with the exact-match scoring protocol. TinyRS-R1 drops to 76.0% because CoT decoding inserts reasoning tokens that might be too complicated for a relatively simpler task, such as yes or no, rural or urban questions.

- On RSVG-DIOR bounding-box grounding, TinyRS-R1 achieves 74.9% precision, outperforming the best existing 7B model by 10% and exceeding the baseline TinyRS by 5.5%. The result suggests that spatial alignment profits from step-by-step token-region reasoning, while remaining insensitive to the shorter answer bias present in VQA.
- Both 2B variants lag behind the Qwen2-VL-RS derivatives on LHRB-Bench, while remaining the best of the rest among other models. TinyRS slightly outperforms its CoT-enhanced counterpart (57.4 vs. 56.8%), suggesting that the additional reasoning tokens did not sufficiently compensate for the general knowledge capacity. This highlights a future need for knowledge augmentation or retrieval strategies at the 2B scale, particularly in light of the performance gain observed in Qwen2-VL-RS-R1 over its non-reasoning variant at 7B scale.

6 Ablation Study

In this work, training is done within four stages. In Table 2, each of these stages are turned off at least three times and their effect is reported.

Effect of remote-sensing pre-training (P). Comparing the model with and without pre-training (Line 4 vs Line 5) shows modest but consistent gains in scene classification, grounding, and rare knowledge questions, with VQA unchanged. These improvements suggest that pre-training helps the model grasp basic aerial image features, aiding later stages without adding size or latency overhead.

Table 2: Ablation study for training baselines. Average scores are provided for CLS and VQA. P: Pre-training, S: SFT, C: CoT SFT, R: GRPO RL

P	S	C	R	CLS	VQA	Ground.	Gen. Know.
✓	✓	✓	✓	85.6	76.0	74.9	56.8
✓	✓	✓	✗	84.7	78.3	70	57.1
✓	✓	✗	✓	82.1	78.4	69.5	55.7
✓	✓	✗	✗	81.0	83.5	69.4	57.4
✗	✓	✗	✗	80.0	83.3	67.7	53.6
✓	✗	✓	✗	71.8	67.7	53.4	46.7
✗	✗	✗	✓	58.7	61.7	16.1	52.3
✗	✗	✗	✗	59.8	62.9	6.7	55.2

Effect of supervised instruction fine-tuning (S). Turning supervised fine-tuning on or off (Line 2 vs Line 6) shows it's the main driver of performance. It boosts all classification, VQA knowledge and grounding tasks significantly. This stage doesn't just improve formatting—it teaches the model what kind of answers to give, laying the foundation for later reasoning or RL.

Effect of Chain-of-Thought fine-tuning (C). Comparing with and without Chain-of-Thought (Line 1 vs Line 3) reveals a trade-off: CoT boosts classification, grounding, and general knowledge, but hurts VQA. This suggests CoT helps with structured tasks but not short-answer ones.

Effect of GRPO reinforcement learning (R). Adding GRPO to a reasoning model (Line 1 vs Line 2) acts as a precision booster by improving grounding significantly and classification modestly, but dropping VQA due to longer answers, like CoT. The minimal change in rare knowledge shows GRPO mainly sharpens spatial accuracy, making it valuable when grounding matters most.

Effect of “cold” GRPO without P, CoT or S. Comparing GRPO-only training to the instruction-tuned baseline Qwen2-VL (Line 7 vs Line 8) shows why staged training matters.

GRPO alone boosts grounding by 9.4%, but hurts all other metrics by overfocusing on IoU at the cost of correct labels and concise answers. Qualitative analysis also reveals that the reasoning generated by the cold-started model is of lower quality and sometimes simply repeats the answer. This confirms GRPO works best after SFT and CoT, and should be skipped as a standalone method for these tasks.

Effect of Accuracy Reward Functions in GRPO. The study explores alternative reward formulations to the standard continuous rewards used for open-ended and visual grounding tasks. Two variants are tested: **(1) Binary reward:** assigns 1 if $\text{IoU} \geq 0.5$ (for grounding) or GPT-4.1-mini score ≥ 0.7 (for open-ended), and 0 otherwise. **(2) Quantized reward:** gives 1 for $\text{IoU}/\text{score} \geq 0.7$, a scaled continuous reward for values between 0.4 and 0.7, and 0 for values ≤ 0.4 , applied to both task types. According to the results in Table 3, while the continuous reward is not the best in every benchmark, it is clearly the best overall. Although the quantized reward never achieves the highest score in any individual benchmark, it consistently delivers balanced performance, making it a reasonable second choice. The binary reward can be used as an alternative when training a task-specific model, such as for classification or general knowledge, but it is not optimal for general-purpose remote sensing tasks.

Effect of Dataset Balancing. To demonstrate the impact of dataset balancing—increasing the sampling weight of certain tasks by replicating specific examples up to five times per epoch during SFT—we repeated the experiments using the original unbalanced dataset. As shown in Table

4, dataset balancing significantly improves the performance of both TinyRS and TinyRS-R1 in classification and VQA tasks, although there is a slight drop in visual grounding and general knowledge scores. Overall, these results clearly indicate that dataset balancing enhances the general performance of the model.

7 Conclusion

This paper introduces TinyRS and TinyRS-R1, the first 2B-parameter multimodal small language models (MSLMs) tailored for remote sensing tasks, providing a practical alternative to large 7B-scale models. By combining domain-specific pretraining, instruction tuning, chain-of-thought (CoT) reasoning, and GRPO-based reinforcement learning, TinyRS-R1 achieves or surpasses the performance of much larger models in classification, visual grounding, and multi-step reasoning—while requiring significantly less computational resources. In contrast, the base TinyRS model, which omits reasoning augmentation, proves advantageous for concise, latency-sensitive VQA tasks. These complementary strengths underscore a trade-off between depth of reasoning and response efficiency, enabling flexible deployment depending on task needs. However, both models still underperform in general remote sensing

Table 3: Ablation study for reward functions of TinyRS-R1. Average scores are provided for CLS and VQA.

Function	CLS	VQA	Ground.	Gen. Know.
Continuous	85.6	76.0	74.9	56.8
Quantized	85.3	74.1	73.6	57.3
Binary	85.9	75.5	72.5	57.7

Table 4: Ablation study for balancing dataset for TinyRS and TinyRS-R1. Average scores are provided for CLS and VQA.

Model	Balanced	CLS	VQA	Ground.	Gen. Know.
TinyRS	✓	81.0	83.5	69.4	57.4
TinyRS	✗	80.5	80.8	70.0	58.1
TinyRS-R1	✓	85.6	76.0	74.9	56.8
TinyRS-R1	✗	80.8	73.2	75.1	57.2

knowledge tasks, highlighting the importance of future research in knowledge augmentation and retrieval-augmented modeling for domain-specialized MSLMs. Overall, TinyRS and TinyRS-R1 establish a new benchmark for compact, domain-adapted remote sensing language models and demonstrate the potential of MSLMs for resource-constrained environments.

Acknowledgements

The numerical calculations reported in this paper were partially performed using the MareNostrum 5 pre-exascale supercomputing system and TÜBİTAK ULAKBİM, High Performance and Grid Computing Center (TRUBA resources). We gratefully acknowledge the Barcelona Supercomputing Center (BSC) and the Scientific and Technological Research Council of Turkey (TÜBİTAK) for providing access to these resources and supporting this research.

References

- [1] Deep Agent. Open-r1v. <https://github.com/Deep-Agent/R1-V>, 2025.
- [2] Jinze Bai, Shuai Bai, Yunfei Chu, Zeyu Cui, Kai Dang, Xiaodong Deng, Yang Fan, Wenbin Ge, Yu Han, Fei Huang, Binyuan Hui, Luo Ji, Mei Li, Chang Zhou, Jingren Zhou, Xiaohuan Zhou, Tianhang Zhu, et al. Qwen technical report, 2023. URL <https://arxiv.org/abs/2309.16609>.
- [3] Jinze Bai, Shuai Bai, Shusheng Yang, Shijie Wang, Sinan Tan, Peng Wang, Junyang Lin, Chang Zhou, and Jingren Zhou. Qwen-vl: A frontier large vision-language model with versatile abilities. *arXiv preprint arXiv:2308.12966*, 2023.
- [4] Yakoub Bazi, Laila Bashmal, Mohamad Mahmoud Al Rahhal, Riccardo Ricci, and Farid Melgani. Rs-llava: A large vision-language model for joint captioning and question answering in remote sensing imagery. *Remote Sensing*, 16(9):1477, 2024.
- [5] Lucas Beyer, Andreas Steiner, André Susano Pinto, Alexander Kolesnikov, Xiao Wang, Daniel Salz, Maxim Neumann, Ibrahim Alabdulmohsin, Michael Tschannen, Emanuele Bugliarello, et al. Paligemma: A versatile 3b vlm for transfer. *arXiv preprint arXiv:2407.07726*, 2024.
- [6] Elliot Bolton, Abhinav Venigalla, Michihiro Yasunaga, David Hall, Betty Xiong, Tony Lee, Roxana Daneshjou, Jonathan Frankle, Percy Liang, Michael Carbin, et al. Biomedlm: A 2.7 b parameter language model trained on biomedical text. *arXiv preprint arXiv:2403.18421*, 2024.
- [7] Tom Brown, Benjamin Mann, Nick Ryder, Melanie Subbiah, Jared D Kaplan, Prafulla Dhariwal, Arvind Neelakantan, Pranav Shyam, Girish Sastry, Amanda Askell, et al. Language models are few-shot learners. *Advances in neural information processing systems*, 33:1877–1901, 2020.
- [8] Martin Juan José Bucher and Marco Martini. Fine-tuned’small’llms (still) significantly outperform zero-shot generative ai models in text classification. *arXiv preprint arXiv:2406.08660*, 2024.

- [9] Zhe Chen, Jiannan Wu, Wenhui Wang, Weijie Su, Guo Chen, Sen Xing, Muyan Zhong, Qinglong Zhang, Xizhou Zhu, Lewei Lu, et al. Internvl: Scaling up vision foundation models and aligning for generic visual-linguistic tasks. In *Proceedings of the IEEE/CVF Conference on Computer Vision and Pattern Recognition*, pages 24185–24198, 2024.
- [10] Mostafa Dehghani, Basil Mustafa, Josip Djolonga, Jonathan Heek, Matthias Minderer, Mathilde Caron, Andreas Steiner, Joan Puigcerver, Robert Geirhos, Ibrahim M Alabdulmohsin, et al. Patch n’pack: Navit, a vision transformer for any aspect ratio and resolution. *Advances in Neural Information Processing Systems*, 36:2252–2274, 2023.
- [11] Matt Deitke, Christopher Clark, Sangho Lee, Rohun Tripathi, Yue Yang, Jae Sung Park, Mohammadreza Salehi, Niklas Muennighoff, Kyle Lo, Luca Soldaini, et al. Molmo and pixmo: Open weights and open data for state-of-the-art multimodal models. *arXiv preprint arXiv:2409.17146*, 2024.
- [12] Jacob Devlin, Ming-Wei Chang, Kenton Lee, and Kristina Toutanova. Bert: Pre-training of deep bidirectional transformers for language understanding. *arXiv preprint arXiv:1810.04805*, 2018.
- [13] Alexey Dosovitskiy, Lucas Beyer, Alexander Kolesnikov, Dirk Weissenborn, Xiaohua Zhai, Thomas Unterthiner, Mostafa Dehghani, Matthias Minderer, Georg Heigold, Sylvain Gelly, et al. An image is worth 16x16 words: Transformers for image recognition at scale. *arXiv preprint arXiv:2010.11929*, 2020.
- [14] Luyu Gao, Aman Madaan, Shuyan Zhou, Uri Alon, Pengfei Liu, Yiming Yang, Jamie Callan, and Graham Neubig. Pal: Program-aided language models. In *International Conference on Machine Learning*, pages 10764–10799. PMLR, 2023.
- [15] Daya Guo, Dejian Yang, Haowei Zhang, Junxiao Song, Ruoyu Zhang, Runxin Xu, Qi-hao Zhu, Shirong Ma, Peiyi Wang, Xiao Bi, et al. Deepseek-r1: Incentivizing reasoning capability in llms via reinforcement learning. *arXiv preprint arXiv:2501.12948*, 2025.
- [16] Edward Hu, Yining Shen, Peter Wallis, Zeyuan Allen-Zhu, Yuanzhi Li, Lijuan Wang, and Weizhu Chen. Lora: Low-rank adaptation of large language models. *arXiv preprint arXiv:2106.09685*, 2022.
- [17] Y Hu, J Yuan, C Wen, X Lu, and X Li. A remote sensing vision language model and benchmark. arxiv 2023. *arXiv preprint arXiv:2307.15266*, 2023.
- [18] Yushi Hu, Weijia Shi, Xingyu Fu, Dan Roth, Mari Ostendorf, Luke Zettlemoyer, Noah A Smith, and Ranjay Krishna. Visual sketchpad: Sketching as a visual chain of thought for multimodal language models. *Advances in Neural Information Processing Systems*, 37:139348–139379, 2025.
- [19] Huggingface. Open-r1. <https://github.com/huggingface/open-r1>, 2025.
- [20] Aybora Koksal and A Aydin Alatan. Milchat: Introducing chain of thought reasoning and grpo to a multimodal small language model for remote sensing. *arXiv preprint arXiv:2505.07984*, 2025.

[21] Kartik Kuckreja, Muhammad Sohail Danish, Muzammal Naseer, Abhijit Das, Salman Khan, and Fahad Shahbaz Khan. Geochat: Grounded large vision-language model for remote sensing. In *Proceedings of the IEEE/CVF Conference on Computer Vision and Pattern Recognition*, pages 27831–27840, 2024.

[22] Chengzu Li, Wenshan Wu, Huanyu Zhang, Yan Xia, Shaoguang Mao, Li Dong, Ivan Vulić, and Furu Wei. Imagine while reasoning in space: Multimodal visualization-of-thought. *arXiv preprint arXiv:2501.07542*, 2025.

[23] Zhenshi Li, Dilxat Muhtar, Feng Gu, Xueliang Zhang, Pengfeng Xiao, Guangjun He, and Xiaoxiang Zhu. Lhrs-bot-nova: Improved multimodal large language model for remote sensing vision-language interpretation. *arXiv preprint arXiv:2411.09301*, 2024.

[24] Hunter Lightman, Vineet Kosaraju, Yuri Burda, Harrison Edwards, Bowen Baker, Teddy Lee, Jan Leike, John Schulman, Ilya Sutskever, and Karl Cobbe. Let’s verify step by step. In *The Twelfth International Conference on Learning Representations*, 2023.

[25] Haotian Liu, Chunyuan Li, Qingyang Wu, and Yong Jae Lee. Visual instruction tuning, 2023.

[26] Zechun Liu, Changsheng Zhao, Forrest Iandola, Chen Lai, Yuandong Tian, Igor Fedorov, Yunyang Xiong, Ernie Chang, Yangyang Shi, Raghuraman Krishnamoorthi, Liangzhen Lai, and Vikas Chandra. Mobilellm: Optimizing sub-billion parameter language models for on-device use cases, 2024. URL <https://arxiv.org/abs/2402.14905>.

[27] LMMs-Lab. Open-r1 multimodal. <https://github.com/EvolvingLMMs-Lab/open-r1-multimodal>, 2025.

[28] Dilxat Muhtar, Zhenshi Li, Feng Gu, Xueliang Zhang, and Pengfeng Xiao. Lhrs-bot: Empowering remote sensing with vgi-enhanced large multimodal language model. In *European Conference on Computer Vision*, pages 440–457. Springer, 2024.

[29] Dilxat Muhtar, Enzhuo Zhang, Zhenshi Li, Feng Gu, Yanglangxing He, Pengfeng Xiao, and Xueliang Zhang. Quality-driven curation of remote sensing vision-language data via learned scoring models. *arXiv preprint arXiv:2503.00743*, 2025.

[30] Maxwell Nye, Anders Johan Andreassen, Guy Gur-Ari, Henryk Michalewski, Jacob Austin, David Bieber, David Dohan, Aitor Lewkowycz, Maarten Bosma, David Luan, Charles Sutton, and Augustus Odena. Show your work: Scratchpads for intermediate computation with language models, 2021. URL <https://arxiv.org/abs/2112.00114>.

[31] OpenAI. Gpt-3.5 turbo fine-tuning and api updates, 2023. URL <https://openai.com/index/gpt-3-5-turbo-fine-tuning-and-api-updates/>.

[32] OpenAI. Gpt-4v(ision) system card, 2023. URL https://cdn.openai.com/papers/GPTV_System_Card.pdf.

[33] OpenAI. Introducing openai o1-preview, 2024. URL <https://openai.com/index/introducing-openai-o1-preview/>.

- [34] OpenAI. Introducing gpt-4.1 in the api, 2025. URL <https://openai.com/index/gpt-4-1/>.
- [35] OpenAI. Openai o3-mini, 2025. URL <https://openai.com/index/openai-o3-mini/>.
- [36] Chao Pang, Xingxing Weng, Jiang Wu, Jiayu Li, Yi Liu, Jiaxing Sun, Weijia Li, Shuai Wang, Litong Feng, Gui-Song Xia, et al. Vhm: Versatile and honest vision language model for remote sensing image analysis. In *Proceedings of the AAAI Conference on Artificial Intelligence*, volume 39, pages 6381–6388, 2025.
- [37] Alec Radford, Karthik Narasimhan, Tim Salimans, Ilya Sutskever, et al. Improving language understanding by generative pre-training. *Technical Report*, 2018.
- [38] Alec Radford, Jong Wook Kim, Chris Hallacy, Aditya Ramesh, Gabriel Goh, Sandhini Agarwal, Girish Sastry, Amanda Askell, Pamela Mishkin, Jack Clark, et al. Learning transferable visual models from natural language supervision. *arXiv preprint arXiv:2103.00020*, 2021.
- [39] Zhihong Shao, Peiyi Wang, Qihao Zhu, Runxin Xu, Junxiao Song, Xiao Bi, Haowei Zhang, Mingchuan Zhang, YK Li, Y Wu, et al. Deepseekmath: Pushing the limits of mathematical reasoning in open language models. *arXiv preprint arXiv:2402.03300*, 2024.
- [40] Andreas Steiner, André Susano Pinto, Michael Tschannen, Daniel Keysers, Xiao Wang, Yonatan Bitton, Alexey Gritsenko, Matthias Minderer, Anthony Sherbondy, Shangbang Long, et al. Paligemma 2: A family of versatile vlms for transfer. *arXiv preprint arXiv:2412.03555*, 2024.
- [41] Gemma Team, Thomas Mesnard, Cassidy Hardin, Robert Dadashi, Surya Bhupatiraju, Shreya Pathak, Laurent Sifre, Morgane Rivière, Mihir Sanjay Kale, Noah Fiedel, Evan Senter, Alek Andreev, Kathleen Kenealy, et al. Gemma: Open models based on gemini research and technology, 2024. URL <https://arxiv.org/abs/2403.08295>.
- [42] Gemma Team, Morgane Riviere, Shreya Pathak, Pier Giuseppe Sessa, Cassidy Hardin, Surya Bhupatiraju, Léonard Hussenot, Thomas Mesnard, Bobak Shahriari, Koray Kavukcuoglu, Clement Farabet, Elena Buchatskaya, Sebastian Borgeaud, Noah Fiedel, Armand Joulin, Kathleen Kenealy, Robert Dadashi, Alek Andreev, et al. Gemma 2: Improving open language models at a practical size, 2024. URL <https://arxiv.org/abs/2408.00118>.
- [43] InternLM Team. Internlm: A multilingual language model with progressively enhanced capabilities. <https://github.com/InternLM/InternLM-techreport>, 2023.
- [44] Hugo Touvron, Thibaut Lavril, Gautier Izacard, Xavier Martinet, Marie-Anne Lachaux, Timothée Lacroix, Baptiste Rozière, Naman Goyal, Eric Hambro, Faisal Azhar, Aurelien Rodriguez, Armand Joulin, Edouard Grave, and Guillaume Lample. Llama: Open and efficient foundation language models, 2023.

[45] Jonathan Uesato, Nate Kushman, Ramana Kumar, Francis Song, Noah Siegel, Lisa Wang, Antonia Creswell, Geoffrey Irving, and Irina Higgins. Solving math word problems with process-and outcome-based feedback. *arXiv preprint arXiv:2211.14275*, 2022.

[46] Ashish Vaswani, Noam Shazeer, Niki Parmar, Jakob Uszkoreit, Llion Jones, Aidan N Gomez, Łukasz Kaiser, and Illia Polosukhin. Attention is all you need. In *Advances in Neural Information Processing Systems*, pages 5998–6008, 2017.

[47] Peiyi Wang, Lei Li, Zhihong Shao, RX Xu, Damai Dai, Yifei Li, Deli Chen, Yu Wu, and Zhifang Sui. Math-shepherd: Verify and reinforce llms step-by-step without human annotations. *arXiv preprint arXiv:2312.08935*, 2023.

[48] Peng Wang, Shuai Bai, Sinan Tan, Shijie Wang, Zhihao Fan, Jinze Bai, Keqin Chen, Xuejing Liu, Jialin Wang, Wenbin Ge, et al. Qwen2-vl: Enhancing vision-language model’s perception of the world at any resolution. *arXiv preprint arXiv:2409.12191*, 2024.

[49] Xuezhi Wang, Jason Wei, Dale Schuurmans, Quoc Le, Ed Chi, Sharan Narang, Aakanksha Chowdhery, and Denny Zhou. Self-consistency improves chain of thought reasoning in language models. *arXiv preprint arXiv:2203.11171*, 2022.

[50] Jason Wei, Xuezhi Wang, Dale Schuurmans, Maarten Bosma, Fei Xia, Ed Chi, Quoc V Le, Denny Zhou, et al. Chain-of-thought prompting elicits reasoning in large language models. *Advances in neural information processing systems*, 35:24824–24837, 2022.

[51] Shunyu Yao, Dian Yu, Jeffrey Zhao, Izhak Shafran, Tom Griffiths, Yuan Cao, and Karthik Narasimhan. Tree of thoughts: Deliberate problem solving with large language models. *Advances in neural information processing systems*, 36:11809–11822, 2023.

[52] Di Zhang, Wei Liu, Qian Tan, Jingdan Chen, Hang Yan, Yuliang Yan, Jiatong Li, Weiran Huang, Xiangyu Yue, Dongzhan Zhou, et al. Chemllm: A chemical large language model. *arXiv preprint arXiv:2402.06852*, 2024.

[53] Wei Zhang, Miaoxin Cai, Tong Zhang, Yin Zhuang, and Xuerui Mao. Earthgpt: A universal multi-modal large language model for multi-sensor image comprehension in remote sensing domain. *IEEE Transactions on Geoscience and Remote Sensing*, 2024.

[54] Zhuosheng Zhang, Aston Zhang, Mu Li, Hai Zhao, George Karypis, and Alex Smola. Multimodal chain-of-thought reasoning in language models. *arXiv preprint arXiv:2302.00923*, 2023.